Neuron
Report

Synaptophysin Regulates the Kinetics of Synaptic Vesicle Endocytosis in Central Neurons

Sung E. Kwon[1] and Edwin R. Chapman[1,*]
[1]Howard Hughes Medical Institute and Department of Neuroscience, University of Wisconsin, Madison, WI 53706, USA
*Correspondence: chapman@physiology.wisc.edu
DOI 10.1016/j.neuron.2011.04.001

SUMMARY

Despite being the most abundant synaptic vesicle membrane protein, the function of synaptophysin remains enigmatic. For example, synaptic transmission was reported to be completely normal in synaptophysin knockout mice; however, direct experiments to monitor the synaptic vesicle cycle have not been carried out. Here, using optical imaging and electrophysiological experiments, we demonstrate that synaptophysin is required for kinetically efficient endocytosis of synaptic vesicles in cultured hippocampal neurons. Truncation analysis revealed that distinct structural elements of synaptophysin differentially regulate vesicle retrieval during and after stimulation. Thus, synaptophysin regulates at least two phases of endocytosis to ensure vesicle availability during and after sustained neuronal activity.

INTRODUCTION

Synaptophysin (syp) was the first synaptic vesicle (SV) protein to be cloned and characterized (Jahn et al., 1985; Navone et al., 1986; Wiedenmann and Franke, 1985), and is now known to belong to a family of proteins with four transmembrane domains that includes synaptogyrin (syg) and synaptoporin (Sudhof et al., 1987). Syp is the most abundant SV protein by mass, accounting for ~10% of total vesicle protein (Takamori et al., 2006). Each SV harbors ~32 copies of syp, which is second only to synaptobrevin (8% of the total SV protein) at ~70 copies per vesicle. Because syp is exclusively localized to SVs, it is widely used as a marker for presynaptic terminals.

Structurally, syp spans the vesicle membrane four times with a short amino- and a long carboxy-terminal tail, both of which are exposed on the cytoplasmic surface of the SV membrane. In addition, there are two short intravesicular loops that contain disulfide bonds. Syp is N-glycosylated on the first intravesicular loop and is phosphorylated on the long cytoplasmic tail; the function of these posttranslational modifications remain unknown (Evans and Cousin, 2005; Pang et al., 1988; Wiedenmann and Franke, 1985). There is evidence suggesting that syp, especially its four transmembrane domains, may promote formation of highly curved membranes as in small SVs (Leube, 1995). Indeed, ectopic expression of syp alone in nonneuronal cells leads to formation of small cytoplasmic vesicles (Leube et al., 1989). A recent electron microscopy study revealed that syp forms hexameric structures that are similar to connexons (Arthur and Stowell, 2007).

Previous molecular studies have hinted at a number of diverse roles for syp in synaptic function including exocytosis, synapse formation, biogenesis, and endocytosis of SVs (Cameron et al., 1991; Eshkind and Leube, 1995; Leube et al., 1989; Spiwoks-Becker et al., 2001; Tarsa and Goda, 2002; Thiele et al., 2000; Thomas et al., 1988). Surprisingly, mice lacking syp were viable and had no overt phenotype (Evans and Cousin, 2005; McMahon et al., 1996). Synaptic transmission, and the morphology or shape of SVs, were not altered in syp knockout (*syp*−/−) mice (Eshkind and Leube, 1995; McMahon et al., 1996). The lack of an obvious phenotype was attributed to redundant expression of syp isoforms such as synaptogyrin (syg) or synaptoporin. Consistent with this notion, mice lacking both syp and syg exhibited diminished long-term potentiation (Janz et al., 1999). Nevertheless, recent genetic screening in human subjects, and behavioral studies in mice, have implicated loss or truncation of syp in mental retardation and/or learning deficits (Schmitt et al., 2009; Tarpey et al., 2009). These new results suggest that syp might play a subtle yet important role in regulating synaptic transmission in neuronal circuits involved in learning and memory.

As alluded to above, it is not clear as to whether syp functions in the SV recycling pathway in central neurons. To test this notion directly, we performed a quantitative analysis of SV recycling in cultured neurons using optical and electrophysiological methods. We show that syp regulates the endocytosis of SVs both during and after sustained neuronal activity via distinct structural determinants. We further show that the observed defects in endocytosis, due to loss of syp, exacerbate synaptic depression and delay the replenishment of releasable SV pools.

RESULTS

Synaptophysin Regulates the Kinetics of Compensatory SV Endocytosis

To determine whether syp functions in the SV recycling pathway, we directly monitored the trafficking of SV proteins tagged with the pH-sensitive GFP, pHluorin (Miesenbock et al., 1998; Sankaranarayanan and Ryan, 2000), in dissociated hippocampal neurons from syp knockout (*syp*−/−) mice. We used two different optical reporters, syt1-pH and SV2A-pH, in which a pHluorin was fused to the intraluminal domain of the SV membrane protein synaptotagmin 1 (syt1) or SV2A, respectively (Fernandez-Alfonso et al., 2006). These reporters were

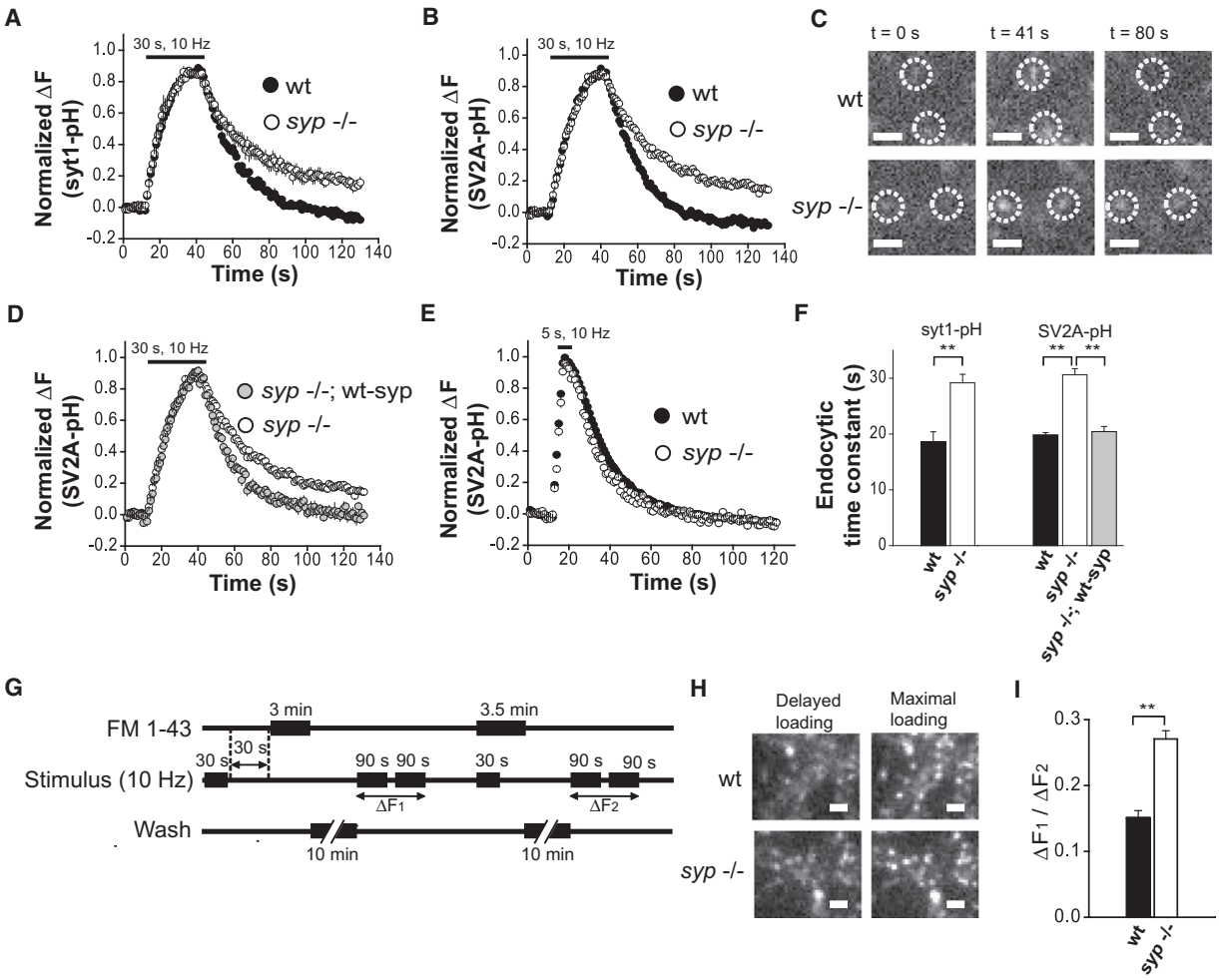

Figure 1. Syp Regulates Endocytosis of SVs after Cessation of Persistent Neuronal Activity

(A) Average traces of wild-type (black) and *syp*−/− (white) neurons expressing synaptotagmin 1-pHluorin (syt1-pH) in response to 300 stimuli at 10 Hz. Average from three coverslips, 20 boutons each. (B) Average traces of wild-type (black) and *syp*−/− (white) neurons expressing SV2A-pHluorin (SV2A-pH) in response to 300 stimuli at 10 Hz. Average from six coverslips, 30 boutons each. (C) Fluorescence images showing presynaptic boutons expressing SV2A-pH in wild-type and *syp*−/− neurons, before stimulation (t = 0) and after cessation of stimulation (t = 41 s or 80 s) at 10 Hz for 30 s. "t" indicates a time point on the horizontal axis of the plot shown in (B). Scale bars represent 2 μm. (D) Average SV2A-pH traces of *syp*−/− (white, six coverslips, 30 boutons each) and wt-syp rescue (gray, five coverslips, 30 boutons each) neurons in response to 300 stimuli at 10 Hz. (E) Average SV2A-pH traces of wild-type (black) and *syp*−/− (white) neurons in response to 50 stimuli at 10 Hz. Average from four coverslips, 40 boutons each. (F) Comparison of average poststimulus endocytic time constants between wild-type, *syp*−/−, and wt-syp rescue neurons. All ΔF values were normalized to the maximal fluorescence intensity change. The decay phases of ΔF traces from syt1-pH or SV2A-pH were fitted with single exponential functions before normalization, and the time constants were calculated from the fits. (G) Protocol for FM1-43 pulse-chase experiments. Neurons were stimulated at 10 Hz for 30 s. After a short delay (30 s), neurons were exposed to FM1-43 for 3 min and then washed in Ca^{2+} solution for 10 min. Two trains of 900 pulses (10 Hz) were delivered to evoke unloading of FM1-43. After a 10 min rest, neurons were stimulated at 10 Hz for 30 s in the presence of FM1-43. This was followed by washing and unloading in the same manner as the first round. (H) Sample images showing boutons labeled with FM1-43 during the delayed loading (left) and the maximal loading (right). Scale bars represent 1.5 μm. (I) Average $\Delta F_1/\Delta F_2$ ratio of wild-type and *syp*−/− neurons. Average from four coverslips, 40 boutons each. All error bars are SEM. **p < 0.001 (two-tailed, unpaired t test throughout).

expressed in neurons using lenti-virus. SV2A-pH is a novel reporter; its use in monitoring the SV cycle in cultured neurons was validated as shown in Figure S1 available online. In short, SV2A-pH is efficiently targeted to recycling SVs and its expression does not interfere with the normal SV recycling pathway (Figures S1A–S1D).

We compared the kinetics of SV endocytosis after sustained stimulation in wild-type (WT) and *syp*−/− neurons. At rest, the fluorescence of syt1-pH remained quenched due to the low pH of the vesicle lumen (pH 5.5) (Figure 1C). Exocytosis, evoked by delivering 300 stimuli (10 Hz), led to a rapid rise in fluorescence due to dequenching of the pHluorin signal upon exposure to the slightly alkaline extracellular solution (pH 7.4), followed by a slow decay due to subsequent endocytosis and reacidification of vesicles (Figures 1A and 1C). Average time constants (τ) of the poststimulus fluorescence decay were significantly greater in *syp*−/− versus WT neurons (τ = 18.6 ± 1.8 s for WT, τ = 29.6 ± 1.5 s for *syp*−/−) (Figures 1A and 1F), indicating slower

SV endocytosis and/or reacidification. To distinguish between these possibilities, we measured the time course of vesicle reacidification and found that the rates were identical in WT (τ = 3.13 ± 1.2 s) versus *syp*−/− neurons (τ = 3.31 ± 1.2 s) (Figure S1E); these time constants are in agreement with previous studies using cultured neurons (Atluri and Ryan, 2006). The slow poststimulus endocytosis in syp−/− neurons was confirmed using SV2A-pH (τ = 19.8 ± 0.5 s in WT, τ = 30.6 ± 1.1 s in *syp*−/−) (Figures 1B and 1F). Direct comparison of these endocytic time constants is valid because the two genotypes have total recycling SV pools of the same size (Figures S1F and S1G). The observed defect in the rate of endocytosis was rescued by expressing wild-type synaptophysin (wt-syp) in *syp*−/− neurons (τ = 20.4 ± 0.9 s in *syp*−/−; wt-syp) (Figures 1D and 1F). Interestingly, when a weaker stimulation protocol was used (50 pulses, 10 Hz), the time course of endocytosis was not significantly different between WT and *syp*−/− neurons (τ = 19.3 ± 0.4 s in WT, τ = 18.5 ± 0.3 s in *syp*−/−) (Figure 1E). Interpretation of this result is provided in the Discussion section.

We performed FM1-43 uptake experiment to test whether SV membrane recycling, in addition to trafficking of cargo proteins, was altered by loss of syp (Figure 1G). WT and *syp*−/− neurons were stimulated in the absence of FM1-43 for 30 s at 10 Hz and, after a 30 s delay, were exposed to the FM dye for 3 min. Neurons were then washed for 10 min in Ca^{2+}-free solution followed by two stimulus trains (900 pulses each at 10 Hz, 2 min rest between two trains) to drive maximal dye release from vesicles. Fluorescence changes (ΔF_1) were measured from images acquired before and after the 900 pulse trains. Each measurement was normalized to a subsequent control run in which FM dye was applied at the onset of stimulus without a delay; this protocol allows labeling the total pool of SVs that undergo exo- and endocytosis during and after the 30 s stimulation, yielding ΔF_2. We hypothesized that, in WT neurons, endocytosis would be largely complete within the 30 s delay, leaving few vesicles available for FM dye uptake (Figures 1A and 1B). However, in *syp*−/− neurons, endocytosis would still be taking place during and after the 30 s delay, resulting in a larger fraction of FM dye-labeled SVs. Indeed, *syp*−/− neurons internalized more dye than wild-type neurons (0.15 ± 0.01 in WT, 0.27 ± 0.01 in *syp*−/−), consistent with slower endocytosis observed using pHluorin (Figures 1H and 1I).

Thus, we conclude that while syp is not essential for endocytosis per se, it is required for kinetically efficient SV retrieval after sustained stimulation.

Syp Regulates Endocytosis during Neuronal Activity

Recent evidence suggests that endocytosis that occurs during sustained stimulation might proceed through molecular mechanisms that are distinct from endocytosis that occurs after stimulation (Ferguson et al., 2007; Mani et al., 2007). As shown above, syp regulates vesicle retrieval after sustained neuronal activity, so we then tested whether syp functions in endocytosis during stimulation. To this end, we took advantage of the vesicular ATPase blocker, bafilomycin (Baf) that inhibits the reacidification of SVs (Nicholson-Tomishima and Ryan, 2004). Neurons expressing SV2A-pH were stimulated at 10 Hz for 30 s in the absence of Baf, and after a 10 min rest, were stimulated again at 10 Hz for a longer time (120 s) in the presence of Baf (Figure 2A). The difference in fluorescence intensity between the two rounds of stimulation reflects the magnitude of endocytosis that had occurred during stimulation (Figure 2B; "Endo") (Nicholson-Tomishima and Ryan, 2004). We derived the time courses of vesicle retrieval during stimulation (labeled as "endocytosis" in Figure 2E) by calculating the difference between the upper (with Baf) and lower (without Baf) traces from each group in Figures 2B–2D. Figure 2E shows the progress of exocytosis and endocytosis during sustained stimulation for all groups. Endocytic rates were empirically estimated from the slope of the time courses (e.g., solid line for WT sample; Figure 2E) (Nicholson-Tomishima and Ryan, 2004). The endocytic rate was decreased by ~4-fold in *syp*−/− (0.014 arbitrary units [AU] s^{-1} in WT, 0.0035 AU s^{-1} in *syp*−/−), and was partially rescued by expressing wt-syp in *syp*−/− neurons (0.0095 AU s^{-1} in *syp*−/−; wt-syp) (Figures 2E and 2F). We also quantified the extent of endocytosis (Endo) as a fraction of exocytosis ("Exo") at the end of the train (t = 43 s). In *syp*−/− neurons, the extent of endocytosis (endo/exo) during sustained neuronal activity was significantly reduced as compared to WT neurons (0.35 ± 0.02 in WT, 0.10 ± 0.03 in *syp*−/−, $p < 0.001$); this defect was rescued by expressing wt-syp in *syp*−/− neurons (0.28 ± 0.03 in *syp*−/−; wt-syp) (Figure 2G). Time courses of exocytosis, estimated by fitting Baf-treated SV2A-pH traces with single exponential functions, were identical in all groups (τ = 31.0 ± 1.2 s in WT, τ = 32.3 ± 1.3 s in *syp*−/−, τ = 32.5 ± 1.8 s in *syp*−/−; wt-syp) (Figure 2H). Therefore, syp is required for efficient SV endocytosis during, as well as after, persistent neuronal activity.

A Cytoplasmic Tail of Synaptophysin Selectively Controls Endocytosis during, but Not after, Neuronal Activity

To understand how syp controls the two phases of SV endocytosis, we focused on the C-terminal cytoplasmic tail that contains putative phosphorylation sites consisting of nine repeats of tyrosine-glycine-proline/glutamine (YG(P/Q) (Sudhof et al., 1987). This tail region was reported to bind dynamin I, which is thought to mediate vesicle fission during endocytosis (Daly and Ziff, 2002; Ferguson et al., 2007). Moreover, injection of a C-terminal fragment of syp into the squid giant axon resulted in accelerated synaptic depression during prolonged stimulation (Daly et al., 2000; Daly and Ziff, 2002).

To address the function of the C-terminal tail of syp, we expressed a mutant syp that lacks this segment (ΔC-syp, lacking amino acids 244–307 that harbor all of the nine YG(P/Q) repeats) in *syp*−/− neurons and analyzed the vesicle retrieval using SV2A-pH. Surprisingly, ΔC-syp rescued the slow poststimulus endocytosis in *syp*−/− neurons to almost the same level as the full-length protein (τ = 20.9 ± 0.7 s in *syp*−/−; ΔC-syp, τ = 20.4 ± 0.9 s in *syp*−/−; wt-syp) (Figure 3A). We then examined vesicle retrieval during stimulation using the same protocol as in Figure 2A (Figure 3B). As compared to wt-syp, the truncation mutant syp failed to rescue defective endocytosis during neuronal activity in terms of rate (0.0095 AU s^{-1} in *syp*−/−; wt-syp, 0.0045 AU s^{-1} in *syp*−/−; ΔC-syp) (Figures 3C and 3D) and the relative magnitude of vesicle retrieval (0.28 ± 0.03 in *syp*−/−; wt-syp, 0.14 ± 0.03 in *syp*−/−; ΔC-syp) (Figures 3B and 3E). These results suggest that the C-terminal domain of

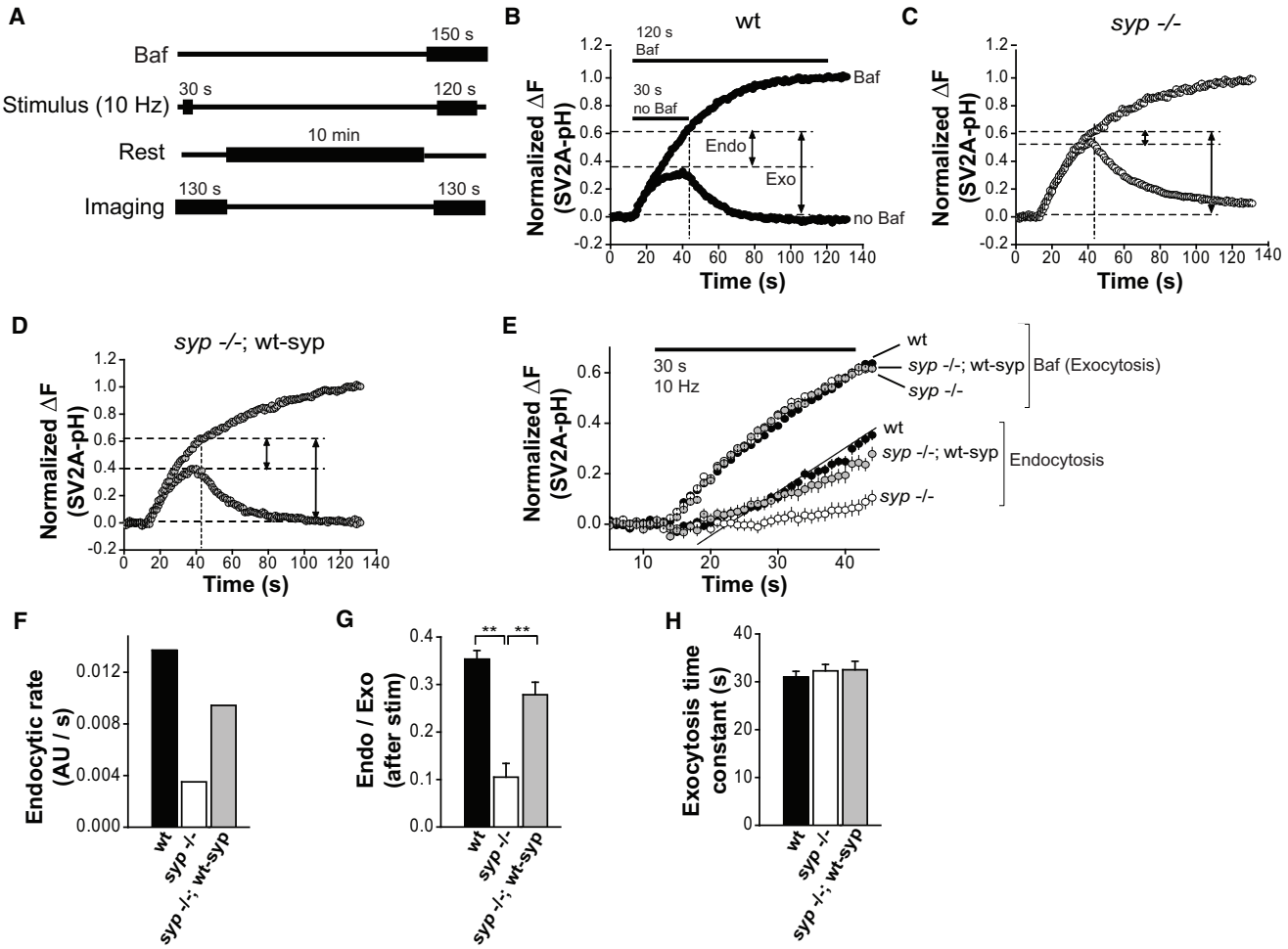

Figure 2. Endocytosis during Sustained Synaptic Transmission Is Reduced in *syp*–/– Neurons

(A) Protocol for measuring time course and extent of endocytosis during neuronal activity using bafilomycin (Baf) to prevent vesicle reacidification. Neurons expressing SV2A-pH were stimulated at 10 Hz for 30 s in the absence of Baf. After a 10 min rest, neurons were stimulated at 10 Hz for 120 s in the presence of Baf. Images were acquired during each phase of stimulation. (B) Average SV2A-pH traces from wild-type neurons in response to 300 stimuli at 10 Hz. Traces represent averages from six coverslips, 30 boutons each. Values were normalized to the maximum fluorescence change at the end of 1200 stimuli in presence of Baf. The short and long arrows (also in C and D) indicate the extent of endocytosis and exocytosis at the end of the 300 stimuli (vertical dashed line) at 10 Hz respectively. (C) The same experiment was repeated in *syp*−/− neurons (six coverslips, 30 boutons each). (D) The same experiment was repeated in wt-syp rescue samples (five coverslips, 30 boutons each). (E) Time courses of exocytosis (Baf) and endocytosis for WT, *syp*−/−, and wt-syp rescue neurons during stimulation (30 s, 10 Hz). Each endocytosis time course was calculated by subtracting the SV2A-pH trace that was acquired in the absence of Baf, from the "Baf" trace in (B) through (D). Endocytosis traces were fitted with linear functions (solid line shown as an example for "WT"). Endocytic rates were determined empirically by calculating slope of the fitted lines. (F) Endocytic rates (in arbitrary units per second [AU/s]) as determined in (E). (G) Average magnitude of endocytosis as a fraction of exocytosis after delivery of 300 pulses. (H) Average exocytic time constants estimated by fitting the rising phase of Baf traces in (B) through (D) with single exponential functions. All error bars represent standard error of the mean (SEM). **$p < 0.001$.

syp is selectively required for the endocytosis that occurs during, but not after, cessation of sustained synaptic transmission.

A previous study reported that the C-terminal tail is essential for internalization of syp in fibroblasts (Linstedt and Kelly, 1991). We tested this notion using full-length pHluorin-tagged synaptophysin (fl sypHy) and the mutant sypHy (ΔC-sypHy) that lacks the same C-terminal segment (amino acids 244–307). ΔC sypHy fluorescence, at the end of the 10 Hz stimulation protocol (30 s), showed a punctate distribution that was indistinguishable from full-length sypHy, reflecting efficient targeting to SVs (Figure S2A). The poststimulus endocytic time-constant of ΔC sypHy (τ = 18.8 ± 0.8 s) was not significantly different from full-length sypHy (τ = 18.0 ± 0.8 s) (Figure S2B), indicating that the C-terminal tail of syp is not required for efficient internalization of syp after neuronal activity. Next, we tested whether trafficking of syp, during neuronal activity, was altered in ΔC sypHy using the same protocol as in Figure 2A. Interestingly, retrieval of ΔC sypHy during neuronal activity was significantly reduced (0.31 ± 0.02 for fl sypHy, 0.18 ± 0.04 for ΔC sypHy) and also became slower as compared to full-length sypHy (0.015 AU s^{-1} for fl sypHy, 0.010 AU s^{-1} for ΔC sypHy) (Figures S2C and S2D). Thus, these results further demonstrate that

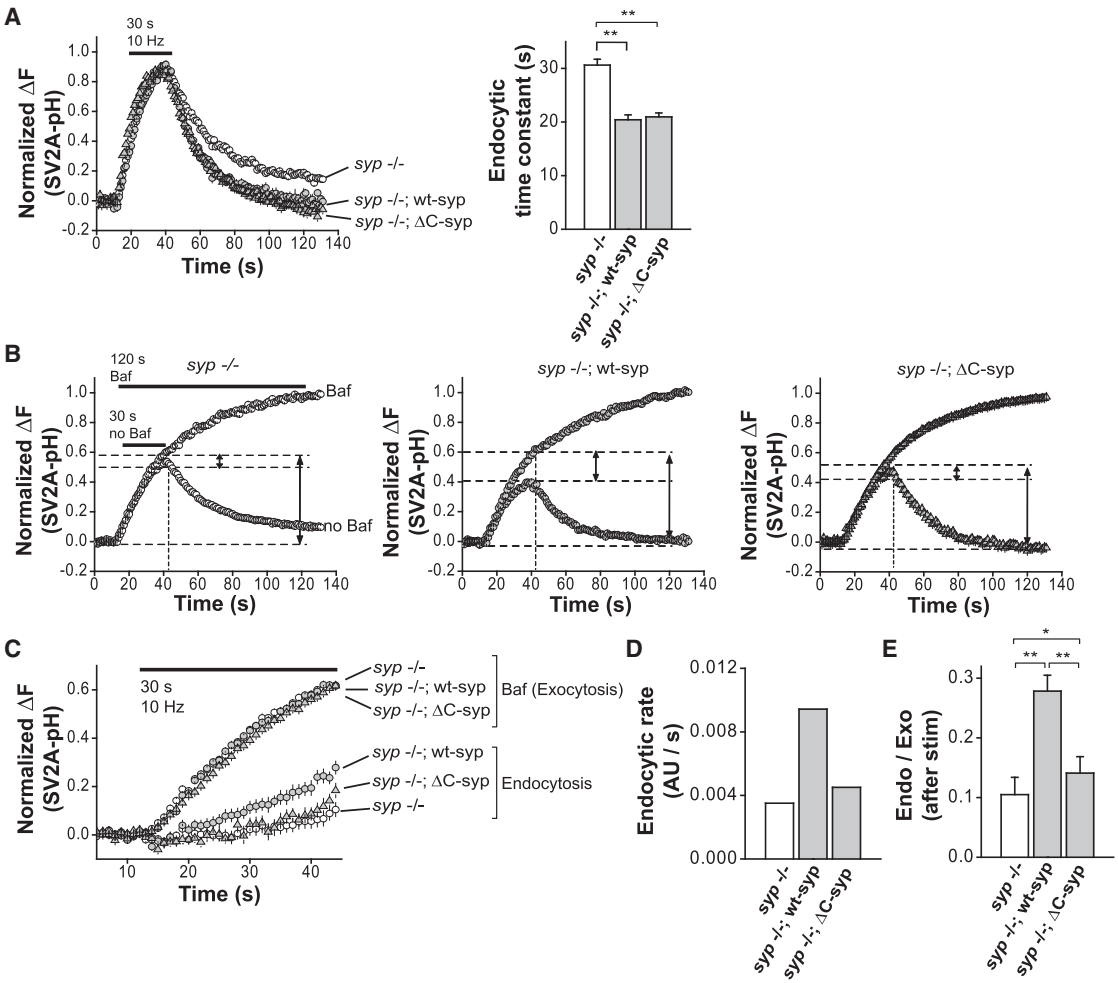

Figure 3. The C-Terminal Cytoplasmic Tail of Synaptophysin Regulates Endocytosis during Persistent Neuronal Activity but Is Not Important for Poststimulus Endocytosis

(A) (Left) Average SV2A-pH traces of *syp−/−* (white, six coverslips, 30 boutons each), wt-syp rescue (black, 5 coverslips, 30 boutons each), and ΔC-syp neurons (gray, five coverslips, 30 boutons each) in response to 300 stimuli at 10 Hz. (Right) Comparison of average poststimulus endocytic time constants between *syp−/−*, wt-syp rescue, and ΔC-syp neurons. (B) Endocytosis during neuronal activity was assayed using the same protocol as shown in Figure 2A. Each trace is an average of the same number of samples as in (A). Time courses of exocytosis (Baf) and endocytosis for *syp−/−* (left), wt-syp rescue (middle), and ΔC-syp neurons (right) during the 30 s stimulation protocol. (C) Time courses of exocytosis (Baf) and endocytosis for *syp−/−*, wt-syp rescue ΔC-syp neurons during the 30 s stimulation at 10 Hz. Each endocytosis time course was calculated by subtracting the SV2A-pH trace that was acquired in the absence of Baf, from the "Baf" trace in each of the three panels in (B). Endocytic rates were determined by fitting the slope with linear functions as in Figure 2E. (D) Endocytic rates (in AU/s) as determined in (C). (E) Average magnitude of endocytosis as a fraction of exocytosis after delivery of 300 stimuli. All error bars represent SEM. *p < 0.05; **p < 0.001.

different motifs within syp are involved in controlling the endocytosis of SV that occurs during, versus after, sustained synaptic transmission, potentially by recruiting distinct ensembles of proteins for recycling.

syp–/– Neurons Exhibit Pronounced Synaptic Depression and a Slower Recovery of the Recycling Vesicle Pool

We investigated the physiological significance of the endocytic defects in *syp−/−* neurons by performing whole-cell voltage-clamp recordings in dissociated cortical neurons. We locally stimulated neurons by delivering electrical pulses to the cell body using a stimulating electrode and recorded evoked inhibitory postsynaptic currents (IPSCs) from the cell body of postsynaptic partners. This method has been used to examine the dynamics of SV pools in numerous studies (Chung et al., 2010; Ferguson et al., 2007). We measured the amplitude and the kinetics of single IPSCs between wild-type and *syp−/−* neurons, and found that these parameters were not altered (Figures S3A and S3B). Short-term plasticity, measured by paired-pulse ratio, was unaltered in *syp−/−* neurons (Figures S3C and S3D). These results suggest that the absence of syp does not affect the neurotransmitter release probability, postsynaptic responses or short-term synaptic plasticity, consistent with a previous study (McMahon et al., 1996).

We then tested whether syp plays a role in maintaining the recycling SV pool during sustained neuronal activity. To this end,

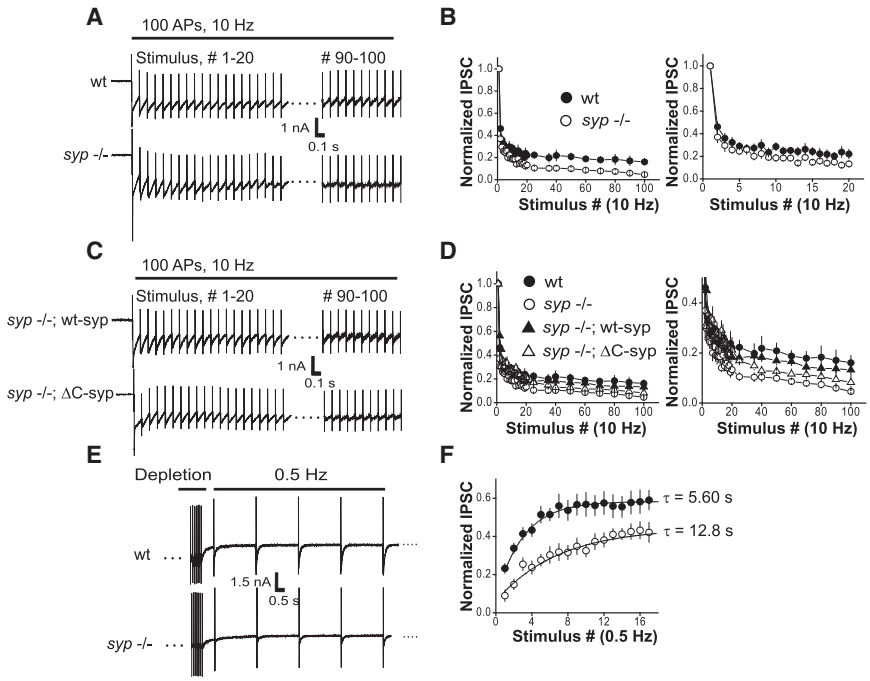

Figure 4. Time Courses of Synaptic Depression and Recovery in *syp–/–* Neurons

(A) Representative traces of evoked inhibitory postsynaptic currents (IPSCs) in WT (top) and *syp*−/− (bottom) during 100 stimuli at 10 Hz in 3 mM Ca^{2+}. (B) (Top) Normalized IPSC amplitudes in WT (black) and *syp*−/− (white) neurons during sustained 10 Hz stimulation. Values are averages from seven WT and seven *syp*−/− neurons. Amplitude values were normalized to the first response in the train. (Bottom) Averages of the first 20 responses during 10 Hz stimulation are shown for clarity. (C) Representative traces of IPSCs in wt-syp (top) and ΔC-syp (bottom) neurons during 100 stimuli at 10 Hz in 3 mM Ca^{2+}. (D) Normalized IPSC amplitudes from wt-syp rescue (gray) and ΔC-syp neurons (gray triangle) are overlaid with WT and *syp*−/− data from (B). Values are averages from eight wt-syp and six ΔC-syp samples. (E) Representative traces of IPSCs from vesicle pool recovery experiments. Neurons were subjected to two separate phases of stimulation: 200 stimuli at 10 Hz in 4 mM Ca^{2+} for maximal depletion of the recycling SV pool, and then a recovery phase with mild stimulation at 0.5 Hz. (F) Normalized IPSC amplitudes from WT (black) and *syp*−/− (white) neurons during the recovery phase. Amplitude values were normalized to the first response in the depletion phase and fitted with single exponential functions. Values are averages from eight WT and eight *syp*−/− neurons. All error bars represent SEM.

we stimulated neurons by delivering a train of 100 pulses at 10 Hz and monitored the depression of IPSCs during the train. The difference between wild-type and *syp*−/− neurons emerged after 20 stimuli and became more pronounced at later time points; by the end of 100 stimuli, only very small IPSCs could be elicited in *syp*−/− neurons, indicating that there were few remaining vesicles ready to fuse (Figures 4A and 4B). The average steady-state amplitudes of the IPSCs, determined by averaging the last 10 responses, were as follows: 0.171 ± 0.04 (WT), 0.060 ± 0.01 (*syp*−/−). The pronounced synaptic depression observed in *syp*−/− neurons was completely rescued by expressing wt-syp (Figures 4C and 4D). In marked contrast, ΔC-syp failed to rescue the enhanced depletion in *syp*−/− neurons (Figures 4C and 4D). Together with findings described above (Figure 3), we conclude that the loss of C-terminal cytoplasmic domain leads to inefficient SV endocytosis and pronounced synaptic depression during sustained neuronal activity.

We also measured the time course of recovery of the recycling SV pool. Neurons were stimulated at 10 Hz for 20 s to deplete vesicles, and after a brief pause, they were stimulated at 0.5 Hz to monitor regrowth of IPSCs (Figure 4E). Amplitudes of all responses were normalized to the first response during the train. Recovery from depletion was significantly slower in *syp*−/− neurons (Figures 4E and 4F). We note that the releasable vesicle pool was not completely depleted in wild-type neurons even with the most intense stimulation that we were able to use without compromising cell viability (200 APs, 10 Hz in 4 mM Ca^{2+}). Nevertheless, recovery proceeds with a much steeper slope in wild-type (τ = 5.60 s), as compared to *syp*−/− neurons (τ = 12.8 s) (Figure 4F), consistent with results from pHluorin experiments shown above.

DISCUSSION

The data reported here firmly establish a role for syp in facilitating rapid and efficient SV endocytosis in mammalian central neurons. *syp*−/− neurons exhibited defective SV endocytosis both during and after neuronal activity while exocytosis and the size of the total recycling pool of SVs were unaffected. Truncation of the C-terminal tail of syp led to slower endocytosis during neuronal activity, consistent with a previous study in which a tail fragment was injected into the squid giant axon (Daly et al., 2000). However, the same truncation mutant had no effect on endocytosis after neuronal activity; hence, the two endocytic processes—one during stimulation and another that is employed after stimulation—are controlled by distinct domains of syp.

The observed defects in SV endocytosis in *syp*−/− neurons result in functional consequences including the pronounced depletion and slower recovery of the recycling SV pool. The slow time constant of poststimulus endocytosis might seem to be at odds with the rapid divergence of the synaptic depression time course between wild-type and *syp*−/− neurons during sustained stimulation (Figures 4A and 4B). Such rapid depression observed in *syp*−/− neurons prompted us to test the possibility that rapid retrieval, or "kiss and run" endocytosis of vesicles, is affected in the absence of syp. We note that whether kiss-and-run/fast retrieval (within ~1 s) is a common mode of endocytosis in hippocampal synapses remains the subject of debate (Balaji et al., 2008; Ertunc et al., 2007; Granseth et al., 2006; Zhang et al., 2009). We calculated the rate of vesicle retrieval that occurs during stimulation as a fraction of the total recycling pool (as

determined by the maximal ΔF values in the Baf traces) (Figures 2E and 2F). For wild-type neurons, only ~1.3% of total recycling pool appears to undergo endocytosis within 1 s; this result argues against the notion that the rapid retrieval (i.e., kiss-and-run) predominates during sustained transmission. Hence, these results indicate that the rapid divergence of the synaptic depression time course between wild-type and *syp*−/− neurons cannot be attributed to loss of putative rapid endocytosis.

An alternative explanation for the pronounced synaptic depression in *syp*−/− neurons is that syp might regulate another relatively rapid step, such as the clearance of vesicle release sites (Neher, 2010). Interactions between SNARE proteins on vesicular and target membranes need to be disrupted after exocytosis to allow vesicle recycling. Syp might facilitate this process by binding to synaptobrevin II and clearing it from active zones. The loss of syp might lead to a "traffic jam" of vesicular components at release sites and thereby contribute to synaptic depression during sustained activity. However, it is not known whether the clearance of release sites is a rate-limiting step in hippocampal synapses. Finally, we note that read-outs from pHluorin imaging experiments and physiological recordings might not be directly comparable with each other due to several technical differences. These include (imaging versus electrophysiology) different methods of stimulating neurons (field stimulation versus local stimulation) and differences in temporal resolution ("s" versus "ms"). Therefore, there are caveats regarding direct comparison of data from these two experimental approaches.

We consider the following possibilities regarding how SV endocytosis can be affected in the absence of syp: (1), unitary endocytic events become slower, or (2), number of SVs that can be retrieved at the same time, i.e., "endocytic capacity" is reduced while endocytosis of individual SVs remains unaffected (Balaji et al., 2008). Since we only measured the macroscopic time courses of vesicle retrieval, we cannot completely distinguish between these two possibilities. Nevertheless, the finding that compensatory vesicle retrieval in *syp*−/− became slower only after 300 stimuli argues the first scenario. Indeed, the rate of unitary endocytic events is reported to be largely invariant (Balaji et al., 2008). Therefore, we propose that the role of syp is to maintain endocytic capacity in synapses. At the molecular level, syp may recruit or promote the assembly of endocytic components in order to maintain the number of available "endocytic machines" during and after sustained neuronal activity.

It will be of interest to determine whether SV endocytosis is further affected in syp and synaptogyrin double knockout mice with impaired long-term potentiation, a neural substrate for learning and memory (Janz et al., 1999). Future studies will also focus on the molecular mechanisms through which syp interacts with binding partners—e.g., synaptobrevin II, dynamin I, and adaptor protein-I—to control vesicle recycling (Daly and Ziff, 2002; Edelmann et al., 1995; Glyvuk et al., 2010; Horikawa et al., 2002). Given that syb II plays a role in vesicle endocytosis and that syp promotes vesicular localization of syb II, it is tempting to speculate that the function of syp in efficient SV endocytosis might involve a physical interaction with syb II (Deak et al., 2004; Hosoi et al., 2009; Wienisch and Klingauf, 2006).

EXPERIMENTAL PROCEDURES

Molecular Biology

Syt1-pH and sypHy constructs were kindly provided by T.A Ryan (New York, NY) and L. Lagnado (Cambridge, UK), respectively. SV2A-pH is described in Supplemental Experimental Procedures.

Neuronal Cultures and Viruses

A syp knock out mouse line was kindly provided by R. Leube (Mainz, Germany) (Eshkind and Leube, 1995). The mouse line was maintained as heterozygous breeding pairs. Primary hippocampal cultures were prepared as described previously in accordance with the guidelines of the National Institutes of Health, as approved by the Animal Care and Use Committee of the University of Wisconsin-Madison (Liu et al., 2009). Viruses were generated in human embryonic kidney 293T cells as previously described (Dong et al., 2006). See Supplemental Experimental Procedures for details.

Live-Cell Imaging

Neurons were continuously perfused with bath solution (140 mM NaCl, 5 mM KCl, 2 mM $CaCl_2$, 2 mM $MgCl_2$, 10 mM HEPES, 10 mM Glucose, 50 μM D-AP5, 10 μM CNQX adjusted to 310 mOsm with glucose, pH 7.4) at room temperature during imaging. During resting or washing steps, the 2 mM Ca^{2+} was replaced with 2 mM Mg^{2+}. For field-stimulation, 1 ms constant voltage pulses (70 V) were delivered digitally using ClampEX 10.0 via two parallel platinum wires spaced by 10 mm in the imaging chamber (Warner Instruments). Time-lapse images taken at 1 s intervals were obtained on an inverted microscope (Nikon TE300) with a 100× oil objective under illumination with a xenon light source (Lambda DG4). Fluorescence changes at individual boutons were detected using a Cascade 512II EMCCD camera (Roper Scientific) with 2 × 2 binning; data were collected and analyzed offline using MetaMorph 6.0 software. See Supplemental Experimental Procedures for details.

Electrophysiology

Whole-cell voltage-clamp recordings of evoked IPSCs were performed using an AxoPatch 200B amplifier (Molecular Devices) driven by pClamp 10. The internal pipette solution contained the following (in mM): 135 $CsCl_2$, 1 EGTA, 10 HEPES, 1 NaGTP, 4 QX-314 (pH 7.4). Cells were continuously perfused with extracellular fluid (ECF): 140 mM NaCl, 5 mM KCl, 3 mM $CaCl_2$, 2 mM $MgCl_2$, 10 mM HEPES, 10 mM Glucose, 50 μM D-AP5, 10 μM CNQX, adjusted to 310 mOsm with glucose, pH 7.4. Recordings with a series resistance significantly larger than 20 MΩ were discarded. When 4 mM Ca^{2+} was used as in Figure 4E, [Mg^{2+}] was lowered to 1 mM. Action potentials were evoked by stimulating presynaptic neurons with a theta-stimulating electrode with a voltage of 20–30 V for 1 ms. Data were sampled at 10 kHz, and filtered at 2 kHz.

SUPPLEMENTAL INFORMATION

Supplemental Information includes three figures and Supplemental Experimental Procedures and can be found with this article online at doi:10.1016/j.neuron.2011.04.001.

ACKNOWLEDGMENTS

We thank M. Jackson and X. Lou for their comments on this manuscript. We also thank M. Dong and M. Dunning for help with cDNA constructs used to carry out this work. This study was supported by a grant from the NIH (MH061876). S.E.K was supported by Epilepsy Foundation predoctoral fellowship. E.R.C is an Investigator of the Howard Hughes Medical Institute.

Accepted: April 1, 2011
Published: June 8, 2011

REFERENCES

Arthur, C.P., and Stowell, M.H. (2007). Structure of synaptophysin: a hexameric MARVEL-domain channel protein. Structure *15*, 707–714.

Atluri, P.P., and Ryan, T.A. (2006). The kinetics of synaptic vesicle reacidification at hippocampal nerve terminals. J. Neurosci. *26*, 2313–2320.

Balaji, J., Armbruster, M., and Ryan, T.A. (2008). Calcium control of endocytic capacity at a CNS synapse. J. Neurosci. *28*, 6742–6749.

Cameron, P.L., Sudhof, T.C., Jahn, R., and De Camilli, P. (1991). Colocalization of synaptophysin with transferrin receptors: implications for synaptic vesicle biogenesis. J. Cell Biol. *115*, 151–164.

Chung, C., Barylko, B., Leitz, J., Liu, X., and Kavalali, E.T. (2010). Acute dynamin inhibition dissects synaptic vesicle recycling pathways that drive spontaneous and evoked neurotransmission. J. Neurosci. *30*, 1363–1376.

Daly, C., and Ziff, E.B. (2002). Ca^{2+}-dependent formation of a dynamin-synaptophysin complex: potential role in synaptic vesicle endocytosis. J. Biol. Chem. *277*, 9010–9015.

Daly, C., Sugimori, M., Moreira, J.E., Ziff, E.B., and Llinas, R. (2000). Synaptophysin regulates clathrin-independent endocytosis of synaptic vesicles. Proc. Natl. Acad. Sci. USA *97*, 6120–6125.

Deak, F., Schoch, S., Liu, X., Sudhof, T.C., and Kavalali, E.T. (2004). Synaptobrevin is essential for fast synaptic-vesicle endocytosis. Nat. Cell Biol. *6*, 1102–1108.

Dong, M., Yeh, F., Tepp, W.H., Dean, C., Johnson, E.A., Janz, R., and Chapman, E.R. (2006). SV2 is the protein receptor for botulinum neurotoxin A. Science *312*, 592–596.

Edelmann, L., Hanson, P.I., Chapman, E.R., and Jahn, R. (1995). Synaptobrevin binding to synaptophysin: a potential mechanism for controlling the exocytotic fusion machine. EMBO J. *14*, 224–231.

Ertunc, M., Sara, Y., Chung, C., Atasoy, D., Virmani, T., and Kavalali, E.T. (2007). Fast synaptic vesicle reuse slows the rate of synaptic depression in the CA1 region of hippocampus. J. Neurosci. *27*, 341–354.

Eshkind, L.G., and Leube, R.E. (1995). Mice lacking synaptophysin reproduce and form typical synaptic vesicles. Cell Tissue Res. *282*, 423–433.

Evans, G.J., and Cousin, M.A. (2005). Tyrosine phosphorylation of synaptophysin in synaptic vesicle recycling. Biochem. Soc. Trans. *33*, 1350–1353.

Ferguson, S.M., Brasnjo, G., Hayashi, M., Wolfel, M., Collesi, C., Giovedi, S., Raimondi, A., Gong, L.W., Ariel, P., Paradise, S., et al. (2007). A selective activity-dependent requirement for dynamin 1 in synaptic vesicle endocytosis. Science *316*, 570–574.

Fernandez-Alfonso, T., Kwan, R., and Ryan, T.A. (2006). Synaptic vesicles interchange their membrane proteins with a large surface reservoir during recycling. Neuron *51*, 179–186.

Glyvuk, N., Tsytsyura, Y., Geumann, C., D'Hooge, R., Huve, J., Kratzke, M., Baltes, J., Boening, D., Klingauf, J., and Schu, P. (2010). AP-1/sigma1B-adaptin mediates endosomal synaptic vesicle recycling, learning and memory. EMBO J. *29*, 1318–1330.

Granseth, B., Odermatt, B., Royle, S.J., and Lagnado, L. (2006). Clathrin-mediated endocytosis is the dominant mechanism of vesicle retrieval at hippocampal synapses. Neuron *51*, 773–786.

Horikawa, H.P., Kneussel, M., El Far, O., and Betz, H. (2002). Interaction of synaptophysin with the AP-1 adaptor protein gamma-adaptin. Mol. Cell. Neurosci. *21*, 454–462.

Hosoi, N., Holt, M., and Sakaba, T. (2009). Calcium dependence of exo- and endocytotic coupling at a glutamatergic synapse. Neuron *63*, 216–229.

Jahn, R., Schiebler, W., Ouimet, C., and Greengard, P. (1985). A 38,000-dalton membrane protein (p38) present in synaptic vesicles. Proc. Natl. Acad. Sci. USA *82*, 4137–4141.

Janz, R., Sudhof, T.C., Hammer, R.E., Unni, V., Siegelbaum, S.A., and Bolshakov, V.Y. (1999). Essential roles in synaptic plasticity for synaptogyrin I and synaptophysin I. Neuron *24*, 687–700.

Leube, R.E. (1995). The topogenic fate of the polytopic transmembrane proteins, synaptophysin and connexin, is determined by their membrane-spanning domains. J. Cell Sci. *108*, 883–894.

Leube, R.E., Wiedenmann, B., and Franke, W.W. (1989). Topogenesis and sorting of synaptophysin: synthesis of a synaptic vesicle protein from a gene transfected into nonneuroendocrine cells. Cell *59*, 433–446.

Linstedt, A.D., and Kelly, R.B. (1991). Endocytosis of the synaptic vesicle protein, synaptophysin, requires the COOH-terminal tail. J. Physiol. (Paris) *85*, 90–96.

Liu, H., Dean, C., Arthur, C.P., Dong, M., and Chapman, E.R. (2009). Autapses and networks of hippocampal neurons exhibit distinct synaptic transmission phenotypes in the absence of synaptotagmin I. J. Neurosci. *29*, 7395–7403.

Mani, M., Lee, S.Y., Lucast, L., Cremona, O., Di Paolo, G., De Camilli, P., and Ryan, T.A. (2007). The dual phosphatase activity of synaptojanin1 is required for both efficient synaptic vesicle endocytosis and reavailability at nerve terminals. Neuron *56*, 1004–1018.

McMahon, H.T., Bolshakov, V.Y., Janz, R., Hammer, R.E., Siegelbaum, S.A., and Sudhof, T.C. (1996). Synaptophysin, a major synaptic vesicle protein, is not essential for neurotransmitter release. Proc. Natl. Acad. Sci. USA *93*, 4760–4764.

Miesenbock, G., De Angelis, D.A., and Rothman, J.E. (1998). Visualizing secretion and synaptic transmission with pH-sensitive green fluorescent proteins. Nature *394*, 192–195.

Navone, F., Jahn, R., Di Gioia, G., Stukenbrok, H., Greengard, P., and De Camilli, P. (1986). Protein p38: an integral membrane protein specific for small vesicles of neurons and neuroendocrine cells. J. Cell Biol. *103*, 2511–2527.

Neher, E. (2010). What is rate-limiting during sustained synaptic activity: vesicle supply or the availability of release sites. Front. Synaptic Neurosci. *2*, 144.

Nicholson-Tomishima, K., and Ryan, T.A. (2004). Kinetic efficiency of endocytosis at mammalian CNS synapses requires synaptotagmin I. Proc. Natl. Acad. Sci. USA *101*, 16648–16652.

Pang, D.T., Wang, J.K., Valtorta, F., Benfenati, F., and Greengard, P. (1988). Protein tyrosine phosphorylation in synaptic vesicles. Proc. Natl. Acad. Sci. USA *85*, 762–766.

Sankaranarayanan, S., and Ryan, T.A. (2000). Real-time measurements of vesicle-SNARE recycling in synapses of the central nervous system. Nat. Cell Biol. *2*, 197–204.

Schmitt, U., Tanimoto, N., Seeliger, M., Schaeffel, F., and Leube, R.E. (2009). Detection of behavioral alterations and learning deficits in mice lacking synaptophysin. Neuroscience *162*, 234–243.

Spiwoks-Becker, I., Vollrath, L., Seeliger, M.W., Jaissle, G., Eshkind, L.G., and Leube, R.E. (2001). Synaptic vesicle alterations in rod photoreceptors of synaptophysin-deficient mice. Neuroscience *107*, 127–142.

Sudhof, T.C., Lottspeich, F., Greengard, P., Mehl, E., and Jahn, R. (1987). A synaptic vesicle protein with a novel cytoplasmic domain and four transmembrane regions. Science *238*, 1142–1144.

Takamori, S., Holt, M., Stenius, K., Lemke, E.A., Gronborg, M., Riedel, D., Urlaub, H., Schenck, S., Brugger, B., Ringler, P., et al. (2006). Molecular anatomy of a trafficking organelle. Cell *127*, 831–846.

Tarpey, P.S., Smith, R., Pleasance, E., Whibley, A., Edkins, S., Hardy, C., O'Meara, S., Latimer, C., Dicks, E., Menzies, A., et al. (2009). A systematic, large-scale resequencing screen of X-chromosome coding exons in mental retardation. Nat. Genet. *41*, 535–543.

Tarsa, L., and Goda, Y. (2002). Synaptophysin regulates activity-dependent synapse formation in cultured hippocampal neurons. Proc. Natl. Acad. Sci. USA *99*, 1012–1016.

Thiele, C., Hannah, M.J., Fahrenholz, F., and Huttner, W.B. (2000). Cholesterol binds to synaptophysin and is required for biogenesis of synaptic vesicles. Nat. Cell Biol. *2*, 42–49.

Thomas, L., Hartung, K., Langosch, D., Rehm, H., Bamberg, E., Franke, W.W., and Betz, H. (1988). Identification of synaptophysin as a hexameric channel protein of the synaptic vesicle membrane. Science *242*, 1050–1053.

Wiedenmann, B., and Franke, W.W. (1985). Identification and localization of synaptophysin, an integral membrane glycoprotein of Mr 38,000 characteristic of presynaptic vesicles. Cell *41*, 1017–1028.

Wienisch, M., and Klingauf, J. (2006). Vesicular proteins exocytosed and subsequently retrieved by compensatory endocytosis are nonidentical. Nat. Neurosci. *9*, 1019–1027.

Zhang, Q., Li, Y., and Tsien, R.W. (2009). The dynamic control of kiss-and-run and vesicular reuse probed with single nanoparticles. Science *323*, 1448–1453.